The Journal of CPRI,
Vol. 9, No. 2, June 2013 pp. 231–240

Low Voltage Ride Through Capability Analysis of DFIG using Feed Forward Current Regulator

Bankar D S* and Talange D B**

In recent years due to increase in the load demand a lot of emphasis is given on the use of non-conventional energy sources since fossil and atomic fuels will not last forever, and that their use contributes to environmental pollution [1]. Out of all non-conventional energy sources wind has been the fastest growing energy source over the last decade mainly due to very significant improvements in wind energy technology. Doubly fed induction generators have become the most popular type of wind turbine generators due to its excellent characteristics of control. But, these types of generators are susceptible to grid-side low voltage faults and short circuits. Power electronics converter connected on the rotor side affects badly under these conditions. When a short circuit or voltage sag occurs on the grid side, the rotor current of the generator tends to rise, which could cause damage to the rotor convert. To overcome this difficulty RSC is disconnected and crow bar is activated thus the DFIG now acts as the conventional induction machine. Grid codes suggest that these plants are required to remain connected to the grid in the event of voltage dip also they should contribute to the power system by feeding the active and reactive power safely [5]. The LVRT requirement is very important as far as grid stability is concern when a large wind farm is connected to the grid. But it is difficult to satisfy for wind plants using DFIG system since the DFIG stator is directly connected to the grid and the rotor is connected through RSC, hence complete DFIG system is much sensitive to grid disturbances [4]. This paper presents the feed forward current regulator for rotor side converter of DFIG and analyses its low voltage ride through capability. The results show that the LVRT capability of doubly fed induction generator has improved.

Keywords: *DFIG, RSC, GSC and LVRT.*

1.0 INTRODUCTION

Wind energy is the most adopted renewable energy among all the sources. In horizontal axis variable speed wind power technology doubly fed induction generators are more popular due to its several advantages on the other types of generator like superior control on the active and reactive power [1, 5]. Also the power electronics connected in the rotor circuit has to handle only 30% of total power hence the harmonics generated by the system are quite low [12]. Also these generators can generate the electricity below as well as above synchronous speed. But DFIG suffers from the drawback that under grid connected system whenever grid side of the generator observes the voltage sag or dip due to any fault on the grid it introduces the DC component in the stator current and causes increase in the DC flux linking with the rotor circuit. Due to this the transient currents are introduced at rotor terminals which have to be handled by the rotor side converter. Therefore

*Associate Professor & Ph.D candidate of Electrical Engineering Department, Bharati Vidyapeeth University College of Engineering, Pune - 411043. E-mail: dsbankar@bvucoep.edu.in.
**Ph.D IIT Bombay, Professor, Electrical Engineering Department, Govt. College of Engineering, Pune-411005, India. E-mail: dbt.elec@coep.ac.in.

RSC has to be over modulated [2, 3, 13]. To handle the situation common technique is to disconnect the RSC in the event of the grid faults and rotor terminals to be connected to the external resistance circuit which is well known as crowbar circuit. Under such circumstances the DFIG now acts as normal induction motor rather than the generator and draws the reactive power from the supply. This happens exactly when the grid needs the reactive power support. A disconnection of large wind farm in such conditions may cause the collapse of the entire grid [5, 7]

The use of crowbar circuit should be the last choice to limit transient rotor currents. This paper proposes a feed-forward current control (FFCC) scheme for the Rotor side converter to enhance the Low voltage ride through capability of DFIGs [9, 14]

2. PROPOSED SYSTEM

2.1 Block Diagram of DFIG System

The basic configuration of a DFIG driven by a wind turbine is shown in Figure 1

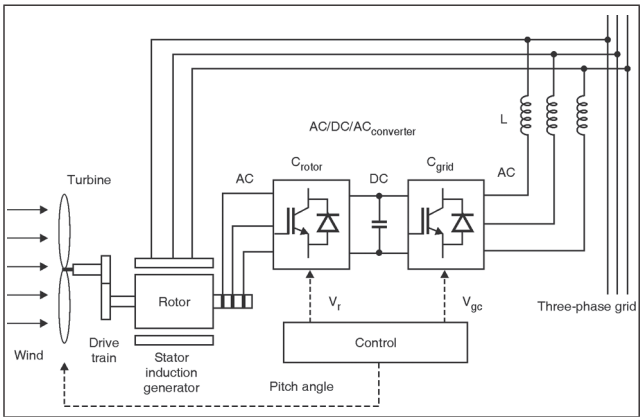

FIG. 1 BLOCK DIAGRAM OF DGIF SYSTEM.

The wind turbine is connected to the DFIG through a mechanical shaft system, with a gearbox in between. The wound rotor induction machine is fed from both stator and rotor sides. The stator is directly connected to the grid while the rotor is connected to the grid through a VFC [8]. The rotor is fed with variable magnitude and variable frequency voltage to keep the stator electrical power at constant voltage and frequency to the utility grid for a wide operating range from sub synchronous to super synchronous speeds. The power flow between the rotor circuit and the grid must be controlled both in magnitude and in direction [15]. Therefore, the VFC consists of two four-quadrant insulated-gate bipolar transistor (IGBT) pulse width modulation (PWM) converters connected back-to-back by a DC-link capacitor. These two converters are called as rotor side converter (RSC) and grid side converter (GSC). The crowbar is used to short circuit the RSC in order to protect it from over current in the rotor circuit during transient grid disturbances. Control of the DFIG is achieved by control of the VFC, which includes control of the RSC [5] and control of the GSC [6].

2.2 Feed Forward Current Regulator

2.2.1 RSC Current Controller

To control the DFIG Rotor side converter and Grid side converter, the conventional vector control scheme is commonly used. The main advantage of this system is that it offers a good decoupled control of the active and reactive power [10].

The *d–q* transformation is adopted for the modeling. The *d–q* convention used assumes that the *q* axis leads the *d*-axis by 90°. Figures 2 and 3 shows the control block diagrams for the rotor side and grid side converters respectively [11]. For controlling the rotor side converter the d-axis is oriented with the stator flux vector, and to control the grid side converter the d-axis is oriented with the stator voltage space vector.

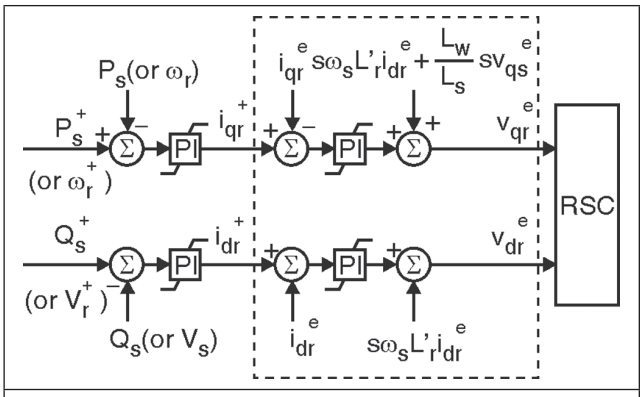

FIG. 2 VECTOR CONTROL SCHEME FOR THE RSC WITH TRADITIONAL FFCR.

The active power or electromagnetic torque is related to the *q*-axis rotor current i^e_{qr} and the reactive power is related to the *d*-axis rotor current i^e_{dr}. This control scheme is known as the feed-forward current regulator. The scheme is derived from a steady state stator voltage and flux condition.

2.2.2 Block Diagrams

The block diagram of the conventional vector control schemes for the RSC and the GSC are shown in Figures 2 and 3 respectively.

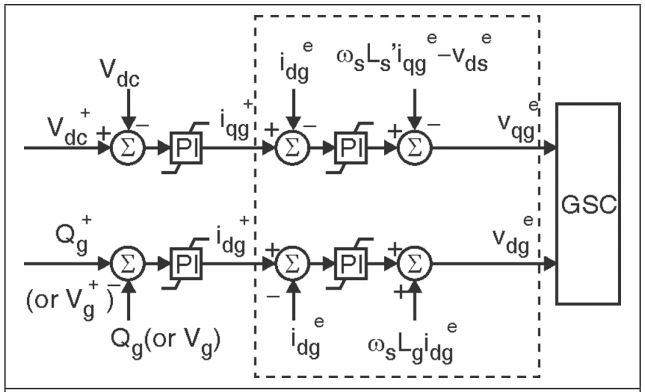

FIG. 3 VECTOR CONTROL SCHEME FOR THE GSC WITH TRADITIONAL FFCR.

2.2.3 Mathematical modeling

The modeling of DFIG is done by considering the arbitrary reference frame. Equation (1) shows the d and q axis stator and rotor voltage respectively. The torque equation can be derived as mentioned in (2)

$$
\begin{aligned}
V_{ds} &= R_s\, i_{ds} + p\varphi_{ds} - \omega\varphi_{ds} \\
V_{qs} &= R_s\, i_{qs} + p\lambda_{qs} + \omega\lambda_{qs} \\
V_{dr} &= R_r\, i_{dr} + p\varphi_{dr} - (\omega - \omega_r)\varphi_{qr} \\
V_{qr} &= R_r\, i_{qr} + p\varphi_{qr} + (\omega - \omega_r)\varphi_{dr} \\
\varphi &= L_s\, i_{ds} + L_m\, i_{dr} \\
\varphi &= L_s\, i_{qs} + L_m\, i_{qr} \\
\varphi &= L_m\, i_{ds} + L_r\, i_{dr} \\
\varphi_{dr} &= L_m\, i_{qs} + L_r\, i_{qr}
\end{aligned}
\qquad \text{....(1)}
$$

$$
T_e = \frac{3\,P\,L_m}{2\,2\,L_s}\left(\varphi_{qs}\, i_{dr} - \varphi_{ds}\, i_{qr}\right) \qquad \text{....(2)}
$$

The φ_s represents the stator flux linkage and the superscript e here denotes the resulting *dq* reference frame and ω is the rotating speed of the arbitrary reference frame. Equations (1) and (2) are valid for steady-state as well as for transient conditions too. When d-axis is continuously attached to the stator flux then we can write as

$$
\varphi^e_{ds} = \varphi_{ms}, \qquad \varphi^e_{qs} = 0 \qquad \text{....(3)}
$$

Therefore, the electromagnetic torque T_e depends only on i^e_{qr} instead of i^e_{dr}. Under this continuous alignment of the d-axis with the stator flux, the rotating speed of the dq reference frame is equal to that of the stator flux at all times, i.e., $\omega(t) = \omega\varphi_s(t)$. During steady state, $\omega\varphi_s$ is equal to the synchronous speed ω_s, However, during stator voltage transients, $\omega\varphi_s$ is not necessarily equal to the synchronous speed. With the instantaneous stator flux orientation, Rs can be neglected and substituting the flux equations into the voltage equations in (1) we get

$$
\begin{bmatrix} v^e_{ds} \\ v^e_{qs} \end{bmatrix} = L_s \begin{bmatrix} p & -\omega\lambda_s \\ \omega\lambda_s & p \end{bmatrix} \begin{bmatrix} i^e_{ds} \\ i^e_{qs} \end{bmatrix} + L_m \begin{bmatrix} p & -\omega\lambda_s \\ \omega\lambda_s & p \end{bmatrix} \begin{bmatrix} i^e_{dr} \\ i^e_{qr} \end{bmatrix} \qquad \text{....(4)}
$$

$$
\begin{bmatrix} v^e_{dr} \\ v^e_{qr} \end{bmatrix} = \begin{bmatrix} R_r + L_r p & -\left(\omega\lambda_s - \omega_r\right) L_r \\ \left(\omega\lambda_s - \omega_r\right) L_r & R_r + L_r p \end{bmatrix} \begin{bmatrix} i^e_{dr} \\ i^e_{qr} \end{bmatrix} + L_m \begin{bmatrix} p & -\left(\omega\lambda_s - \omega_r\right) \\ \left(\omega\lambda_s - \omega_r\right) & p \end{bmatrix} \begin{bmatrix} i^e_{ds} \\ i^e_{qs} \end{bmatrix} \qquad \text{....(5)}
$$

$$
\begin{bmatrix} v^e_{dr} \\ v^e_{qr} \end{bmatrix} = \begin{bmatrix} R_r + L'_r p & -\left(\omega\lambda_s - \omega_r\right) L'_r \\ \left(\omega\lambda_s - \omega_r\right) L'_r & R_r + L_r p \end{bmatrix} \begin{bmatrix} i^e_{dr} \\ i^e_{qr} \end{bmatrix} + \frac{L_m}{L_s} \begin{bmatrix} v^e_{ds} \\ v^e_{qs-}\omega_r\lambda^e_{ds} \end{bmatrix} \qquad \text{....(6)}
$$

Where L^1_r is the rotor transient inductance, $L^1_r = \sigma L_r = 1\text{-}L^2_m / (L_s L_r)$.

Equation (6) gives the instantaneous values of the stator and rotor voltages to the rotor *dq* currents in both steady-state and transient conditions. By integrating the stator voltages the stator flux in (6) could be estimated. Equation (6) gives the necessary rotor terminal voltage up to the RSC ratings when grid fault occurs and causes voltage dip. Therefore the rotor current is controlled.

Under steady-state stator voltage conditions, $\omega\varphi_s = \omega_s$. By neglecting R_s from (1) and (3), the stator voltage equations at steady-state conditions are given by

$$v^e_{ds} = 0, v^e_{qs} = \omega_s \lambda^e_{qs} \quad ....(7)$$

Further by substituting above equation in (6), the steady state model can be derived as

$$\begin{bmatrix} v^e_{dr} \\ v^e_{qr} \end{bmatrix} = \begin{bmatrix} R_r + L'_r p & -s\omega L'_r \\ s\omega L'_r & R_r + L'_r p \end{bmatrix} \begin{bmatrix} i^e_{dr} \\ i^e_{qr} \end{bmatrix} + s\frac{L_m}{L_s} \begin{bmatrix} 0 \\ v^e_{qs} \end{bmatrix} \quad (8)$$

The feed-forward compensation terms in a Feed Forward Current Regulator are based on (8). In this scheme, the d and q axis rotor current control loops are decoupled by feed forward injecting the cross-coupling current terms and the stator voltage coupling term. The d-axis (or q-axis) rotor current PI regulator then directly outputs the d-axis (or q-axis) current related term $R_r + L^1_r p$ and regulates the d-axis (or q-axis) current to its reference value.

2.2.4 Rotor Side Converter (RSC) scheme

The objective of the RSC is to independently regulate the stator active and reactive powers, which are represented by *Ps* and *Qs*, respectively. The reactive-power control using the RSC can be applied to keep the stator voltage *Vs* within the desired range, when the DFIG feeds into a weak power system without any local reactive compensation. When the DFIG feeds into a strong power system, the command of *Qs* can be simply set to zero.

2.2.5 Overall Vector Control Scheme for RSC

Figure 4 shows the overall vector control scheme of the RSC. In order to achieve independent control of the stator active power P_s and reactive power Q_s by means of rotor current regulation, the instantaneous three-phase rotor currents i_{rabc} are sampled and transformed to *d–q* components i_{dr} and i_{qr} in the stator-flux-oriented reference frame. The reference values of i_{dr} and i_{qr} can be determined directly from Q_s and P_s commands, respectively. The actual *d–q* current signals (i_{dr} and i_{qr}) are then compared with their reference signals (i^*_{dr} and i^*_{qr}) to generate the error signals, which are passed through two PI controllers to form the voltage signals v_{dr1} and v_{qr1}. The two voltage signals (v_{dr1} and v_{qr1}) are compensated by the corresponding cross-coupling terms (v_{dr2} and v_{qr2}) to form the *d–q* voltage signals v_{dr} and v_{qr}. These are then used by the PWM module to generate the IGBT gate control signals to drive the rotor side IGBT convertor.

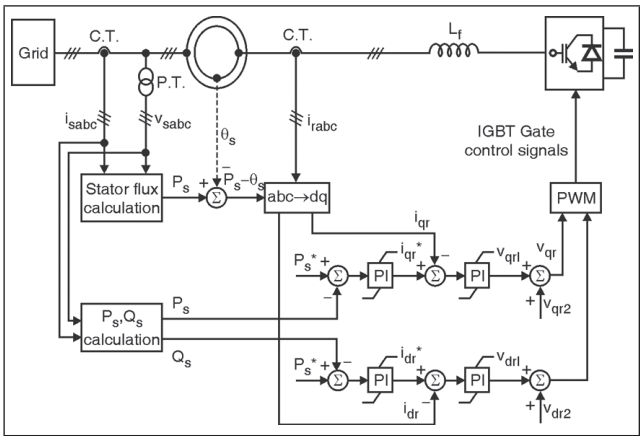

FIG. 4 OVERALL CONTROL SCHEME OF THE ROTOR SIDE CONVERTOR (RSC).

2.3 Grid Side Converter (GSC) control scheme

The objective of the GSC is primarily to keep the DC-link voltage constant regardless of the magnitude and direction of the rotor power. Also when the RSC is blocked, the GSC can be set to

control the reactive power exchange between the DFIG and the grid. Figure 5 shows the overall vector control scheme of the GSC.

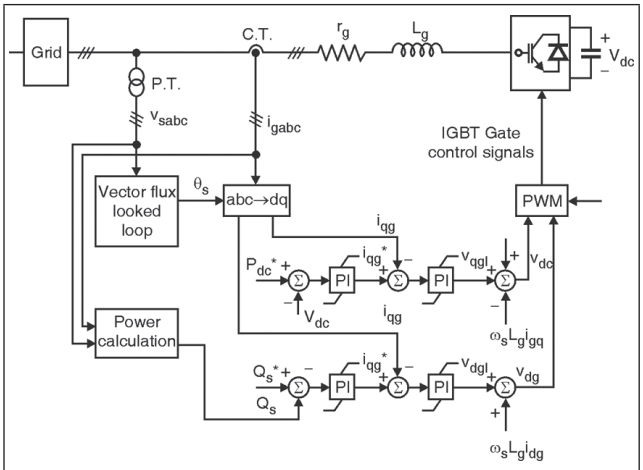

FIG 5 OVERALL CONTROL SCHEME OF THE GRID SIDE CONVERTOR (GSC).

3.0 MATLAB IMPLEMENTATION OF PROPOSED MODEL

The parameters set for the simulation are as follows:

Stator resistance	0.05 p.u.	Nominal Mechanical output	1.5×10^6
Stator leakage reactance	0.1 p.u.	Base wind speed	12 m/s
Rotor resistance	0.02 p.u.	Base rotational speed	1 p.u.
Magnetising inductance	5 p.u.	Base power of electrical generator	1.5×10^6 /0.9
Rotor leakage inductance	0.1 p.u.		
Base frequency	2 × pi ×50	Generator inertia constant	1 s
Turbine inertia constant	5 s	Shaft compliance constant	0.4 p.u./ rad

Figure 6 shows the MATLAB implementation of proposed model.

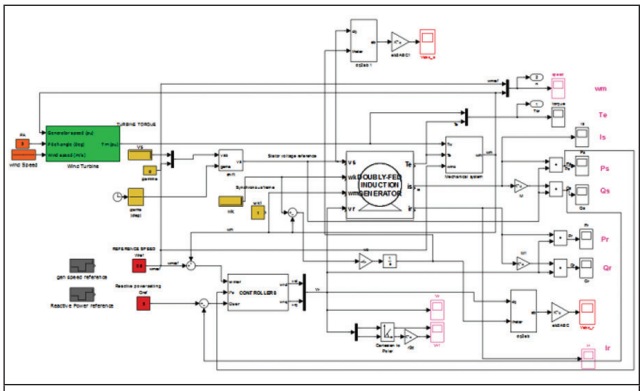

FIG. 6 MATLAB IMPLEMENTATION OF PROPOSED MODEL.

4.0 SIMULATION RESULTS & ANALYSIS

As per the problem discussed in the above sections, the model shown in the Figure 6 is developed to analyze the low voltage ride through capability of the DFIG system using feed forward current regulator for the rotor side converter. Various conditions are set and the model is simulated to obtain the various results. Some conditions with their results are discussed in the following section. Balanced voltage sag of 0.9 p.u., 0.7 p.u., 0.6 p.u., 0.5 p.u., 0.3 p.u. on the grid is set and the various results are captured. Out of which three voltage sag conditions are presented here (viz. 0.7 p.u., 0.5 p.u. and 0.3 p.u.). The duration of the sag is from 10–10.2 sec.

Stator volatge, stator current, rotor current, active power, reactive power, torque and rotor speed are shown in Figures 7–9 for different voltage sag conditions.

Case 1 – Voltage Sag : 0.7 p.u.

The main components to observe from the results are Stator current, rotor current, speed, and active and reactive power contributed by the DFIG along with the settling time of the DFIG after clearance of the fault. The various parameters of the DFIG under grid fault condition (0.7 p.u. voltage sag). Figure 7(a) shows the grid/stator voltage having 0.7 p.u. sag.

Corresponding stator current is shown in Figure 7(b) where the rise in the stator current is about

1.6 p.u. similarly Figure 7(c) shows the rotor current. The rise in the stator current and rotor current is for very small duration and is within the safe limit. Also this current dies out very fast and settles to its normal value quickly.

Active and reactive power contributed by the DFIG during this condition is shown in Figures 7(d) and 7(e) respectively. Figures 7(f) and 7(g) shows the oscillations in the torque and rotor speed respectively and the values are within the limit.

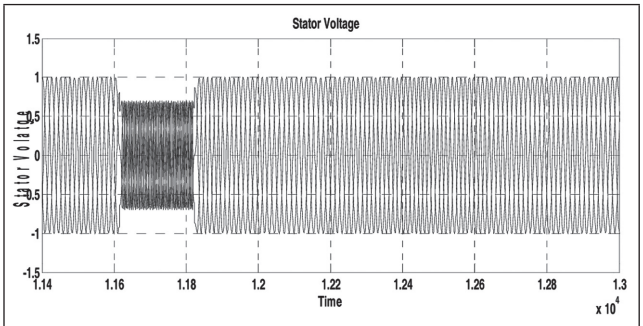

FIG. 7(A) STATOR VOLTAGE.

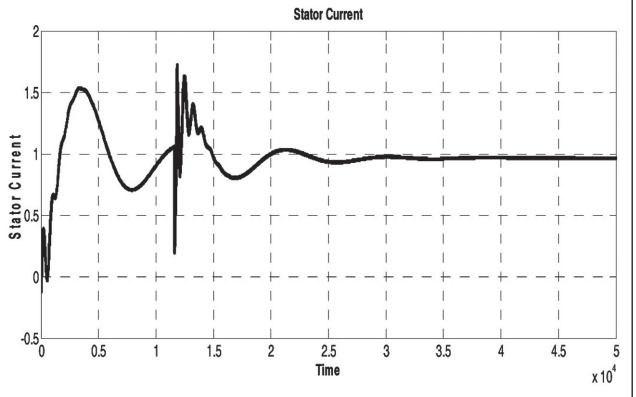

FIG. 7(B) STATOR CURRENT.

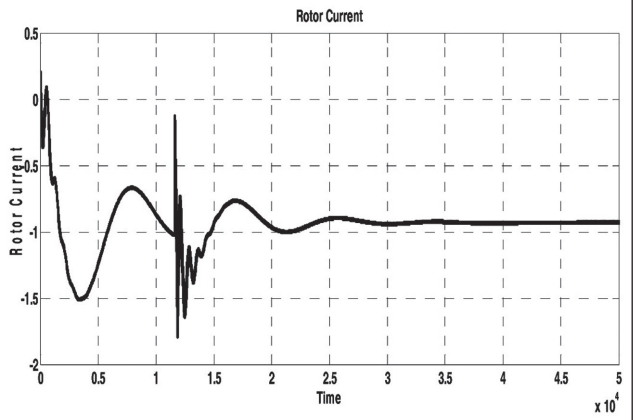

FIG. 7(C) ROTOR CURRENT.

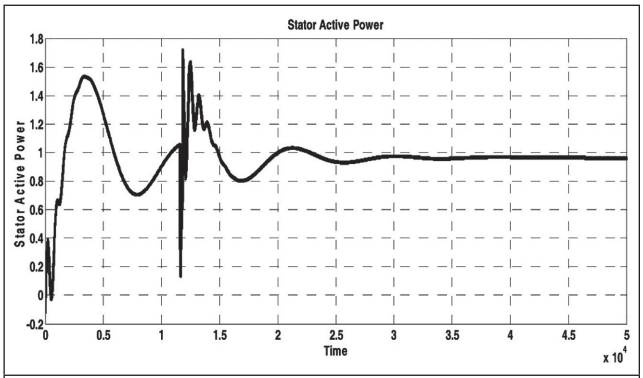

FIG. 7(D) ACTIVE POWER.

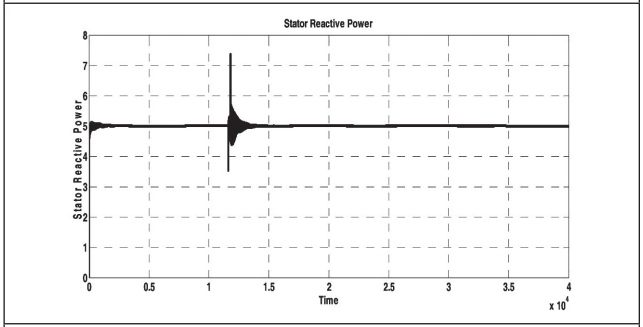

FIG. 7(E) REACTIVE POWER.

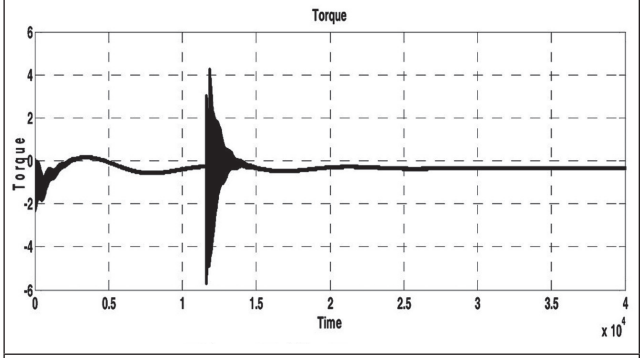

FIG. 7(F) TORQUE.

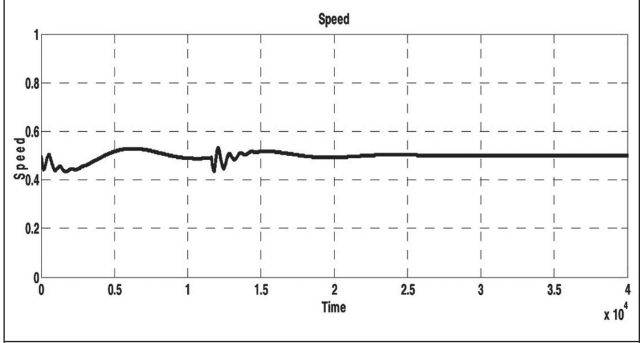

FIG. 7(G) ROTOR SPEED.

FIG. 7 DFIG PERFORMANCE AT 0.7 p.u. VOLTAGE SAG.

Case 2 :Voltage Sag 0.5 p.u.

Above figure shows the various parameters of the DFIG under grid fault condition having 0.5 p.u. voltage sag. Figure 8(a) shows the

grid/stator voltage having 0.5 p.u. sag. Corresponding stator current is shown in Figure 8(b) where the rise in the stator current is about 2.1 p.u. similarly Figure 8(c) shows the rotor current. The rise in the stator current and rotor current is for small duration and is just reach to the unsafe limit. Since these currents dies out very fast and settles to its normal value quickly no immediate harm to the system. Active and reactive power contributed by the DFIG during this condition is shown in Figures 8(d) and 8(e) respectively. Figures 8(f) and 8(g) shows the oscillations in the torque and rotor speed respectively and the values of torque has rise considerably which may oscillate the system at greater amplitude and may damage the rotor and turbine system.

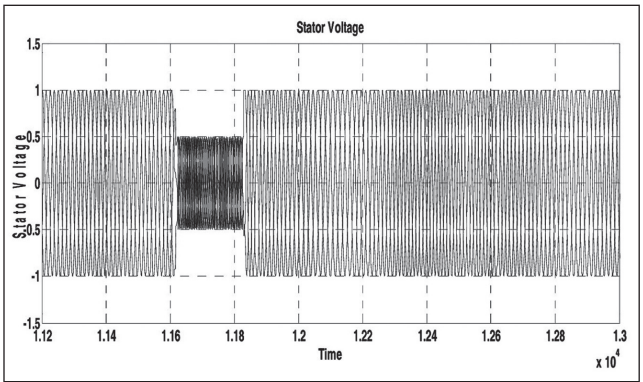

FIG. 8(A) STATOR VOLTAGE.

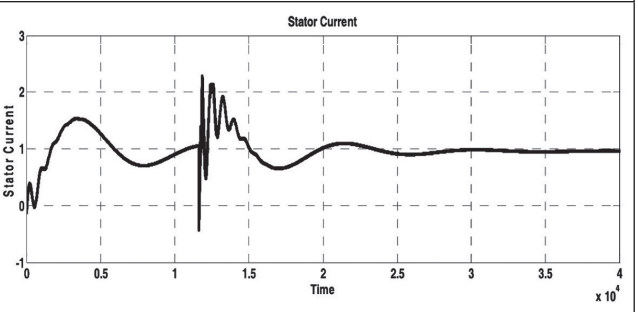

FIG. 8(B) STATOR CURRENT.

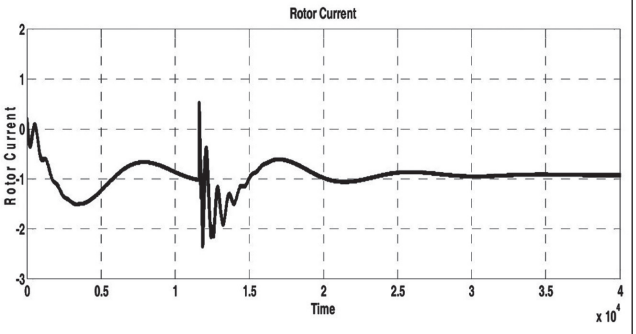

FIG. 8(C) ROTOR CURRENT.

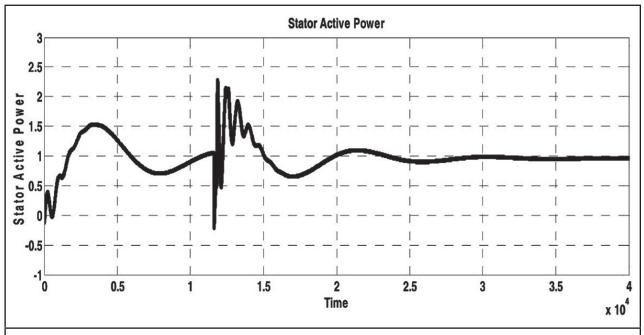

FIG. 8(D) ACTIVE POWER.

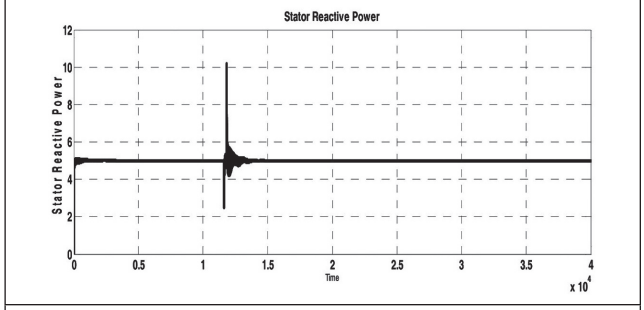

FIG. 8(E) REACTIVE POWER.

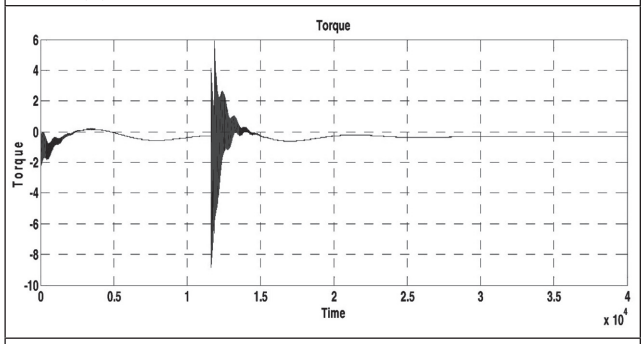

FIG. 8(F) TORQUE.

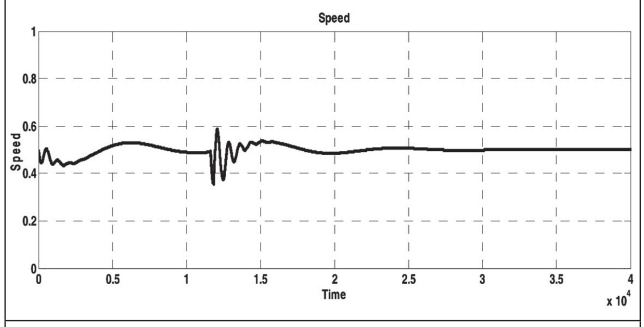

FIG. 8(G) SPEED.

FIG. 8 DFIG PERFORMANCE AT 0.5 p.u. VOLTAGE SAG.

Case 3: Voltage Sag 0.3 p.u.

Figure 9 shows the various parameters of the DFIG under grid fault condition having 0.3 p.u. voltage sag. All the parameters of the DFIG has rise to unsafe magnitude. Figure 9(a) shows the grid/stator voltage having 0.5 p.u. sag and corresponding stator current is shown in Figure 9(b) where the rise in the stator current is about

2.3 p.u. and oscillates between –ve and +ve values. Similarly Figures 9(c) and 9(d) shows the rotor current and rotor voltage, where current magnitude has raised to 2.5 p.u. and voltage magnitude has raised to 5.2 p.u.. The rise in the stator current and rotor current is for longer duration and RSC and GSC need to be disconnected from the system to protect against such transient currents. Also the torque Figure 9(e) and the speed Figure 9(f) fluctuations are tremendously large and thus it may damage the mechanical system. The rotor active power (Figure 9(g)) also reached to unsafe values.

Figure 9(h) indicates the active power handled by the stator durng fault condition where it oscillates between –1.34 PU to 2.3 PU simillerly figure 9 (i) indicates the reactive power of the stator which oscillated between –2 PU to more than 8 PU. These conditions are unsafe for the system.

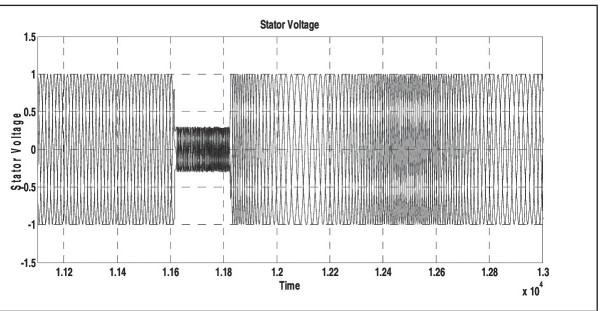

FIG. 9(A) STATOR VOLTAGE.

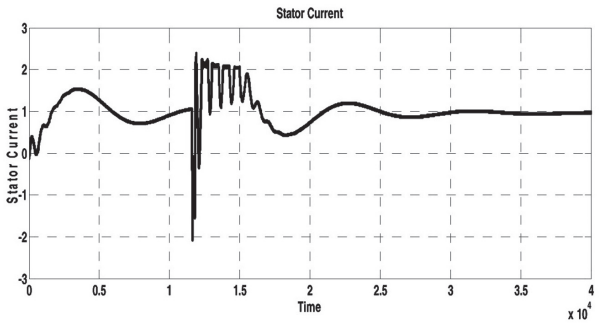

FIG. 9(B) STATOR CURRENT.

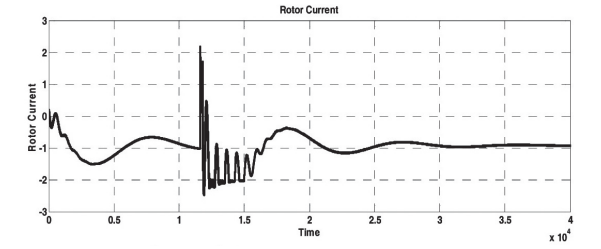

FIG. 9(C) ROTOR CURRENT.

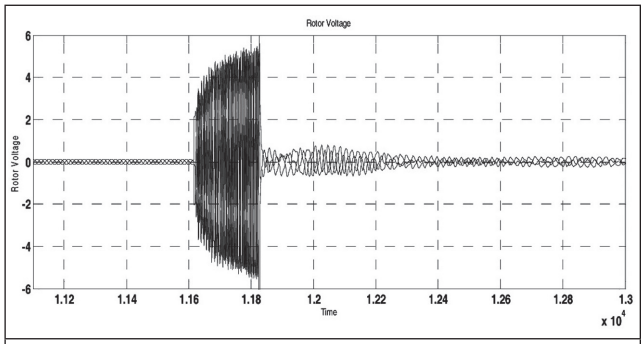

FIG. 9(D) ROTOR VOLTAGE.

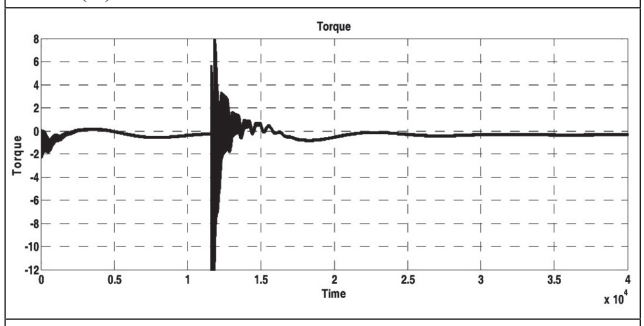

FIG. 9(E) TORQUE.

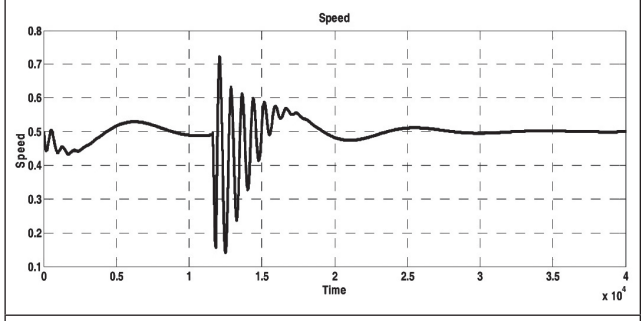

FIG. 9(F) SPEED.

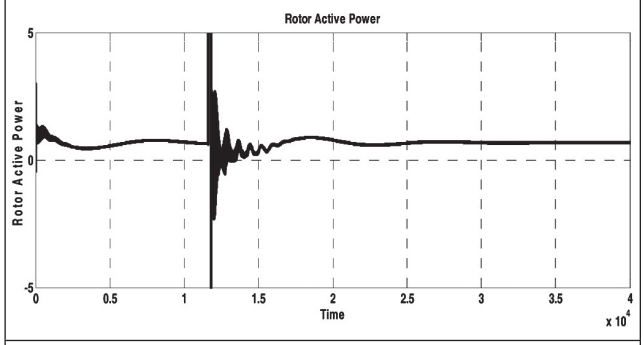

FIG. 9(G) ROTOR ACTIVE POWER.

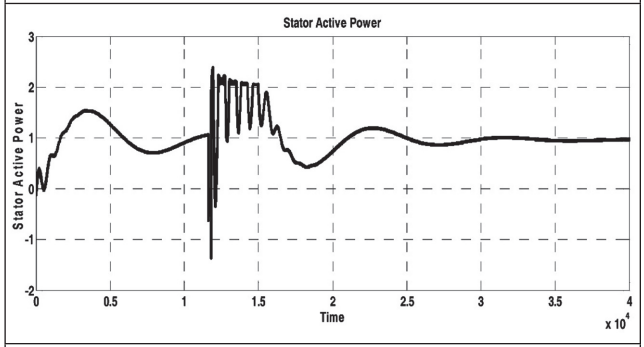

FIG. 9(H) ACTIVE POWER.

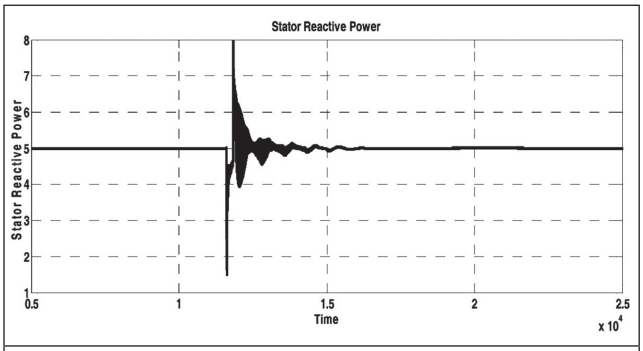

FIG. 9(I) REACTIVE POWER.

FIG. 9 DFIG PERFORMANCE AT 0.3 p.u. VOLTAGE SAG

5.0 CONCLUSION

When the wind turbines are equipped with the Doubly Fed Induction Generator then it is difficult to satisfy the low voltage ride through capability. Therefore uninterrupted power supply is difficult especially in voltage sag condition. An attempt is made to design the feed forward current regulator for the rotor side converter to limit the transients occurring in the rotor side power electronics. From the results it is observed that the low voltage ride through capability of Doubly Fed Induction Generator is considerably improved than the normal regulator and it may avoid the abrupt interruption of the Doubly Fed Induction Generator under grid fault condition. It also minimizes the operation of crowbar circuit during the voltage sag condition and gives an uninterrupted reactive power support to the grid. It helps doubly fed induction generators to remain in operation even during severe grid faults (0.5 p.u.).

REFERENCES

[1] Qiao W and Harley R G. "Grid connection requirements and solutions for DFIG wind turbines," in *Proc. IEEE Energy 2030 Conf.*, Atlanta, GA, November 17–18, pp. 1–8, 2008.

[2] Federal Energy Regulatory Commission. (2005, January 2). Regulatory Order No. 661: Interconnection for Wind Energy. Online: http://www.ferc.gov/industries/electric/indus-act/gi/wind.

[3] Lopez J, Sanchis P, Roboam X and Marroyo L. "Dynamic behavior of the doubly fed induction generator during 3-phase voltage dips," *IEEE Trans. Energy Convers.*, Vol. 22, No. 3, pp. 709–717, September 2005.

[4] Morren J and de Hann S W H. "Ride through of wind turbines with doubly-fed induction generator during a voltage dip," *IEEE Trans. Energy Convers.*, Vol. 20, No. 2, pp. 435–441, June 2005.

[5] Erlich I, Wrede H and Feltes C. "Dynamic behavior of DFIG based wind turbines during grid faults," in *Proc. Power Convers. Conf. (PCC 2007)*, Nagoya, Japan, April 2–5, pp. 1195–1200, 2007.

[6] Abbey C and Joos G. "Supercapacitor energy storage for wind energy applications," *IEEE Trans. Ind. Appl.*, Vol. 43, No. 3, pp. 769–776, May/June 2005.

[7] Qiao W, Zhou W, Aller J M and Harley R G. "Wind speed estimation based sensorless output maximization control for a wind turbine driving a DFIG," *IEEE Trans. Power Electron.*, Vol. 23, No. 3, pp. 1156–1169, May 2008.

[8] Lorenz R and Lawson D. "Performance of feed forward current regulators for field-oriented induction machine controllers," *IEEE Trans. Ind. Appl.*, Vol. IA-23, No. 4, pp. 597–602, July/August 1985.

[9] Muljadi E, Butterfield C P, Parsons B and Ellis A. "Effect of variable speed wind turbine generator on stability of a weak grid," *IEEE Trans. Energy Convers.*, Vol. 22, No. 1, pp. 29–36, March 2005.

[10] Muyeen S M, Takahaski R, Ali M H, Murata T and Tamura J. "Transient stability augmentation of power system including wind farms by using ECS," *IEEE Trans. Power Syst.*, Vol. 23, No. 3, pp. 1179–1187, August 2008.

[11] Munteanu, Bacha S, Bratcu A I, Guiraud J and Roye D. "Energy reliability optimization of wind energy conversion systems by

sliding mode control," *IEEE Trans. Energy Convers.*, Vol. 23, No. 3, pp. 975– 985, September 2008.

[12] Shahabi M, Haghifam M R, Mohamadian M. "Microgrid dynamic performance improvement using a doubly fed induction wind generator," *IEEE Trans. Energy Convers.*, Vol. 24, No. 1, pp. 137–145, March 2009.

[13] Pak L F and Dinavahi V. "Real-time simulation of a wind energy system based on the doubly-fed induction generator," *IEEE Trans. Power Syst.*, Vol. 24, No. 3, pp. 1301–1309, August 2009.

[14] Ong C.-M. "Dynamic simulation of electric machiner using MATLAB-smulink". *Englewood Cliffs*, NJ: Prentice-Hall, 1998.

[15] Sybille G, Dessaint L A, Giroux P, Dessaint L A, Fortin-Blanchette H, Semaille and Mercier P. "Sympower systems for use with Simulink user guide version 4, *Hydro-Quebec Trans. Energie Technologies*, Montreal, QC, Canada, 2002.